A Novel High-temperature Pressure Sensor Based on Graphene Coated by Si3N4

Zeng, Simei; Tang, Chenggang ; Hong, Hao; Yuan, Fang ; Li, Yuning ; Wang, Yuqiang; Kong, Lingbing ; Sun, Jingye ; Zhu, Mingqiang ; Deng, Tao

DOI
10.1109/JSEN.2022.3232626

Publication date
2023

Document Version
Final published version

Published in
IEEE Sensors Journal

A Novel High-Temperature Pressure Sensor Based on Graphene Coated by Si_3N_4

Simei Zeng, Chenggang Tang, Hao Hong, Yuan Fang, Yuning Li, Yuqiang Wang, Lingbing Kong, Jingye Sun, Mingqiang Zhu, and Tao Deng

***Abstract*—The high-temperature pressure sensors have wide applications in aerospace, petroleum, geothermal exploration, automotive electronics, and other fields. However, the traditional silicon-based pressure sensors are restricted to pressure measurement under 120 °C and cannot be satisfied to measure the pressure of various gases or liquids in high temperature and other harsh environments. This article proposes a novel high-temperature pressure sensor based on graphene, in which a rectangular cavity is applied to improve the piezoresistive characteristics of the sensor. The unique of this sensor is that the graphene is coated by the silicon nitride (Si_3N_4) membrane, which could avoid the oxidation of graphene in high temperature and increase the temperature tolerance range. The sensor was placed at various temperatures (50 °C–420 °C) to explore the temperature characteristics, achieving a maximal temperature coefficient of resistance (TCR) of 0.322% $°C^{-1}$. Moreover, the sensor with a 64 × 9 μm^2 cavity has a high pressure sensitivity of 5.32 × 10^{-4} kPa^{-1}, enabling a wide range from 100 kPa to 10 Pa. Experimental results indicate that the proposed sensor possesses superior pressure sensitivity, a wide pressure detection range, and a high-temperature tolerance of 420 °C, which provides new insight into fabricating high-temperature pressure sensors based on graphene and creates more applications in different fields.**

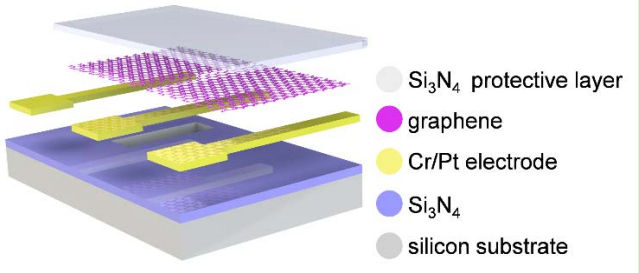

***Index Terms*—Graphene, high temperature, piezoresistive characteristic, silicon nitride (Si_3N_4).**

I. Introduction

THE high-temperature pressure sensors have wide applications in aerospace, petroleum, geothermal exploration, and so on. Currently, pressure sensors are mainly based on diffused silicon (Si). Silicon is a widely used material in integrated circuits due to its relatively mature processing technology, low cost, and excellent device performance [1]. However, on account of the temperature limitation of the p-n junction, the sensor performance will be greatly affected and even failed when working at temperatures higher than 120 °C. When the temperature rises above 500 °C, diffused silicon will produce leakage current and even creep deformation, leading to irreversible changes in Si. Traditional pressure sensors based on diffused silicon are difficult to meet the demands of pressure measurement in high-temperature environments [2]. It is necessary to find new pressure-sensitive materials that can withstand high temperatures and take certain protective arrangement to obtain high-temperature pressure sensors with high performance.

Due to outstanding physical and chemical properties of high carrier mobility, high Young's modulus, and extraordinary thermal conductivity, graphene has great potential to achieve high-temperature pressure sensors with great performance [3], [4], [5]. Graphene is a 2-D honeycomb lattice formed by sp^2 orbital hybridization, which determines that graphene is one of the materials with the highest strength (Young's modulus is 1 TPa) [6]. Graphene has more than 20% reversible elastic deformation [7], and the opening of graphene bandgap could be regulated by stress under uniaxial stress of more than 23% [8]. Moreover, graphene could block standard gas molecules, including helium [9], which is well suited for pressure sensor applications. Meanwhile, the six-membered ring formed by the sp^2 hybrid connection has strong bond energy, which enables graphene to remain stable at thousands of temperatures. Theoretical and experimental results show that the thermal conductivity of monolayer graphene (MLG) reaches 5300 W/mK [5]. In the absence

Manuscript received 25 November 2022; revised 11 December 2022; accepted 11 December 2022. Date of publication 4 January 2023; date of current version 31 January 2023. This work was supported in part by the Fundamental Research Funds for the 173 project under Grant 2020-JCJQ-ZD-043, in part by the project under Grant 22TQ0403ZT07001, in part by the National Natural Science Foundation of China under Grant 61604009 and Grant 61901028, and in part by the Special Research Project on Laboratory Safety under Grant sysaqztyb202117. The associate editor coordinating the review of this article and approving it for publication was Dr. Eui-Hyeok Yang. *(Corresponding author: Tao Deng.)*

Simei Zeng, Chenggang Tang, Yuan Fang, Yuning Li, Yuqiang Wang, Lingbing Kong, Jingye Sun, Mingqiang Zhu, and Tao Deng are with the School of Electronic and Information Engineering, Beijing Jiaotong University, Beijing 100044, China (e-mail: 20120020@bjtu.edu.cn; 20120013@bjtu.edu.cn; 19120004@bjtu.edu.cn; 21111010@bjtu.edu.cn; 21125098@bjtu.edu.cn; 21111095@bjtu.edu.cn; jysun@bjtu.edu.cn; mqzhu@bjtu.edu.cn; dengtao@bjtu.edu.cn).

Hao Hong is with the Department of Microelectronics, Delft University of Technology, 2628 CD Delft, The Netherlands (e-mail: honghao@tsinghua.edu.cn).

Digital Object Identifier 10.1109/JSEN.2022.3232626

of oxygen, graphene can work well at the high temperatures of 2100 °C [10].

To date, vast amounts of research on graphene pressure sensors have been reported. Schedin et al. [11] found that graphene can detect tiny deformations induced by gas molecules attached to its surface. Bunch et al. [12] created the first suspended graphene pressure sensor prototype with multilayer graphene films on a cavity. However, its structure was simple, and it was not a formal component. Smith et al. [13] found a linear correlation between pressure and resistance of the suspended graphene pressure sensor compared with the sensor without a closed cavity, which indicated that the cavity has a great impact on the sensitivity of the graphene pressure sensor. But, the sensor was poorly consistent and did not protect graphene, which can easily cause the device failing quickly. Li et al. [14] proposed a pressure sensor based on graphene/boron nitride (BN). BN was served as the substrate of graphene, which was beneficial to reduce phonon scattering on the graphene surface and increase the mean free path of carriers. Nevertheless, the resistance of the open-faced graphene pressure sensor changed by 41.4% over eight months. Li et al. [15] analyzed the influence of the existence of a cavity on the temperature characteristics of the BN/graphene/BN pressure sensors. However, the sensor without a protective layer can only operate at 30 °C–180 °C, and the temperature coefficient of resistance (TCR) is not high. Graphene is easily doped by oxygen and impurities during the actual manufacturing process, resulting in unstable electrical properties [16], [17]. Besides, graphene is susceptible to thermal stress, structural deformation, or even failure due to temperature. It is important to introduce a protective layer on top of the graphene to insulate it from harsh environments, including high temperature.

Many researchers chose polymers as a protective layer. Kim et al. [18] utilized poly (methylmethacrylate) (PMMA)/polybutadiene (PBU) protecting graphene; however, the device failed after 36 days. Seo et al. [19] employed graphene as an electrode and polydimethylsiloxane (PDMS) polymer as a protective layer to make a photodetector; nonetheless, the effective working time was only 70 h. Another potential material for protecting graphene is silicon nitride (Si_3N_4). It has ultrahigh mechanical strength, ultralow loss [20], and excellent thermal shock characteristics [21]. In addition, Si_3N_4 has good chemical stability and can effectively isolate graphene from oxygen and water molecules [23]. Moreover, the contact between Si_3N_4 and graphene leads to n-type doping, which would improve the electrical performance [22], [23], [24]. Su et al. [25] used Si_3N_4 to package and protect the graphene field-effect transistors (GFET). Within two months, the resistance fluctuation of the GFET was very small.

In this article, a novel low-pressure sensor based on graphene is presented for high-temperature environment. The linear piezoresistive characteristics of the pressure sensor are determined by the pressure-sensitive material of graphene, which also supplies the deformation recovery ability. Meanwhile, to increase the temperature tolerance range, the Si_3N_4 layer is applied to protect graphene from excessive pressure and high-temperature oxidation. The temperature tolerance limitation of the graphene pressure sensor is investigated by using the muffle furnace and other instruments. The sensor can withstand a high temperature of 420 °C with a high TCR of 0.332% $°C^{-1}$ at 150 °C. Also, the influence of different cavity sizes on the piezoresistive characteristics of the sensor is investigated. The experimental results show that when the dimension of the cavity is $64 \times 9\ \mu m^2$, the highest sensitivity of around $5.32 \times 10^{-4}\ kPa^{-1}$ is achieved. Moreover, the piezoresistive characteristics of the graphene pressure sensor at different temperatures are studied. The results show that the resistance of the graphene pressure sensor is positively correlated with temperature and negatively linearly correlated with the applied pressure. Different from pressure sensors based on silicon [27], [28], carbon nanotubes [29], and graphene materials [13], [30], [31], the designed graphene pressure sensor with the Si_3N_4 protective layer exhibits better performance and can work under high temperatures, which paves a new approach for the development of high-temperature pressure detections.

II. Experiments

The fabrication process for the graphene high-temperature pressure sensor coated by Si_3N_4 with a rectangular cavity is shown in Fig. 1. First, the silicon wafer was boiled at 85 °C for 15 min with hydrogen peroxide and sulfuric acid solution (H_2O_2:H_2SO_4 = 1:4), followed by rinsed with deionized water to remove impurities on the surface. Then, a Si_3N_4 passivated layer with a thickness of 200 nm was grown on silicon wafer by low-pressure chemical vapor deposition (LPCVD). AZ601 was used as the mask, and both the Si_3N_4 and Si layers were etched by inductively coupled plasma (ICP) to form a rectangular cavity with a depth of 700 nm. Si_3N_4 was etched by the mixture gas of C_4F_8 (10 sccm) and CF_4 (30 sccm), and Si was etched by the mixture gas of O_2 (2 sccm), SF_4 (9 sccm), and HBr (91 sccm), respectively. Subsequently, chromium/platinum (Cr/Pt) source and drain electrodes with the thicknesses of 10 and 50 nm were sputtered on top of the Si_3N_4 layer. Next, purchased a single layer of graphene grown by chemical vapor deposition (ACS Material, LLC) with a PMMA layer over it from XFNANO. The transfer process was as follows: 1) gently dripped the water around the graphene and allowed it soak in the water slowly; 2) held the edge of the graphene and slowly put it into the water; 3) immersed graphene in water for 2 h; 4) used the Si/Si_3N_4 substrate to pick up the graphene vertically and slowly; 5) after transferred, the substrate was stood for 30 min to remove most of the moisture, and then baked in an oven at 100 °C for 20 min; and 6) cleaned three times with acetone to remove PMMA. The graphene was then graphitized by photolithography and oxygen plasma etching. Finally, a Si_3N_4 protective layer with a thickness of 100 nm was grown by plasma-enhanced chemical vapor deposition (PECVD), and the high-temperature pressure sensor was obtained.

The structure and morphology of graphene pressure sensors were characterized by scanning electron microscopy (FEI Quanta 200 ESEM FEG). The intensity and position changes of the characteristic peaks for graphene before and after covering Si_3N_4 were analyzed by Raman spectroscopy (LabRam HR-800, Horiba Jobin Yvon). The current–voltage (I–V) behavior of the device was measured by a semiconductor parameter analyzer (B1500A, Keysight) and a probe station (Summit 12000, Cascade). After the wafer was cut into small pieces, the graphene pressure sensors were fixed to a ceramic plate with heat resistant glue. The electrode pads were connected to a printed circuit board (PCB) through gold wires. The temperature characteristics of the sensor were investigated by placing the sensor into a muffle furnace (TN-M1700), and the resistance was measured by a multimeter. In order to explore its piezoresistive characteristics under

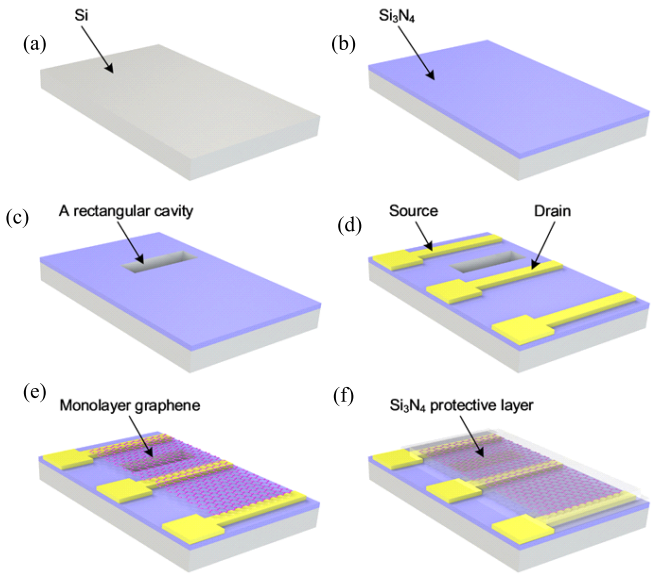

Fig. 1. Fabrication process for the graphene pressure sensor coated by a Si_3N_4 layer with a rectangular cavity. (a) Preclean silicon substrate. (b) Grow Si_3N_4 passivation layer by LPCVD. (c) Etch Si_3N_4 and Si by ICP to form a rectangular cavity. (d) Sputter Cr/Pt source and drain electrodes. (e) Transfer and pattern of the MLG. (f) Deposit a 100-nm Si_3N_4 protective layer.

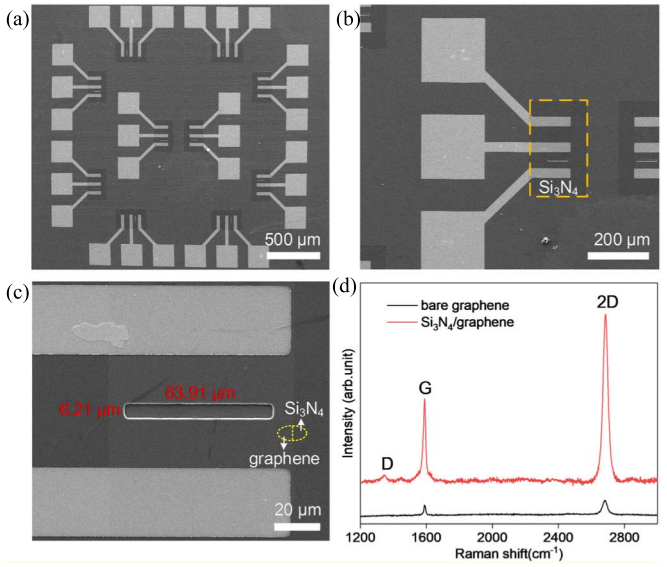

Fig. 2. SEM images and Raman spectroscopy. (a) SEM image for a whole chip containing graphene pressure sensors with a rectangular cavity and temperature sensor without a cavity. (b) Enlarged image of the middle devices. (c) Zoomed-in view for the rectangular cavity is covered by the graphene/Si_3N_4. (d) Raman spectroscopy for the bare graphene and graphene coated by Si_3N_4.

different temperatures, the sensor should be placed in a closed chamber. The temperature and pressure within the chamber were controlled by a low-temperature probe platform (Lake Shore, CRX-4X) and a mechanical pump.

III. Results and Discussion

Fig. 2 shows the SEM images of the graphene pressure sensor with a closed rectangular cavity. The whole chip containing 20 graphene sensing elements is shown in Fig. 2(a), from which it can be seen that there are two types of graphene sensors used in the devices. One is a pressure sensor with a rectangular cavity, while the other is a temperature sensor without a cavity. An enlarged image of the middle devices of the chip is shown in Fig. 2(b). It is worth noting that the electrode in the middle is shared by a pressure sensor and a temperature sensor. As the yellow dashed box indicates that the Si_3N_4 protective layer completely covers the graphene to isolate the external environment. Fig. 2(c) shows an enlarged image for one of the graphene pressure sensing elements. The exact dimension of the cavity is measured as $63.91 \times 6.21\ \mu m^2$ ($L \times W$). It can be seen that the graphene and Si_3N_4 protective layer sit well on top of the pressure cavity.

Raman spectroscopy is utilized to identify the number of graphene layers and quantify information such as disorder. There are three Raman characteristic peaks for graphene, which are D peak (1350 cm^{-1}), G peak (1583 cm^{-1}), and 2-D peaks (2680 cm^{-1}). D peak is the disordered vibration peak of graphene, which is related to the structural defects of graphene. G peak can well display the in-plane vibration of sp^2 carbon atoms, while 2-D peak shows the stacking mode of carbon atoms between layers. The relative strength of the 2-D peak decreases with the increase in graphene layers [32]. The characteristic peak of Si_3N_4 is below 1000 cm^{-1} [33], but three Raman characteristic peaks for graphene are seen above 1300 cm^{-1}, and the passivation layer of Si_3N_4 is below graphene. Therefore, the characteristic peaks of graphene are emphasized in the Raman spectroscopy test, and the spectrum range is 1200–3000 cm^{-1}. The Raman spectroscopy of the graphene on top of the cavity with a Si_3N_4 protective layer and the bare graphene are shown in Fig. 2(d). The G and 2-D peaks of the bare graphene are seen at 1587.85 and 2681 cm^{-1}, respectively. The intensity of the Raman spectrum shifts up as a whole after the graphene pressure sensor was encapsulated by the Si_3N_4 layer. Besides, the G and 2-D peaks shift to the right, which are 1590.1 and 2685.8 cm^{-1}, respectively. The intensity ratio I_{2-D}/I_G is increased from 1.29 to 1.79, attributed to the structural defect caused by the incorporation of heterogeneous nitrogen atoms into the graphene layer [34]. As can be seen from the spectrum, the strength of the D peak is very weak, indicating a high quality of graphene.

Fig. 3 shows the temperature characteristic curves of the graphene pressure sensors with and without Si_3N_4 protection when heating up and cooling down under atmospheric pressure. Six samples were measured, and every sensor was heated up and cooled down for three times. The temperature of Muffle furnace was controlled by the PID program, and the resistance was recorded every 10 °C. During the test, when the temperature exceeded 230 °C, the resistance of the bare graphene pressure sensor began to decrease rapidly, and the device consistency was very poor. Thus, the temperature output characteristic curve of the bare graphene pressure sensors from 50 °C to 230 °C is shown in Fig. 3(a). Fig. 3(b) shows the variation in normalized resistance of the pressure sensors based on Si_3N_4/graphene against the temperature ranging from 50 °C to 420 °C. It can be seen that as the temperature increases, the resistance of both sensors increases, suggesting that they both have a positive temperature coefficient (PTC). During the heating-up process, the temperature-sensitive properties of graphene are mainly affected by the electron–phonon coupling and the thermal expansion effect of graphene/substrate. Electron–phonon coupling mechanism is that when the

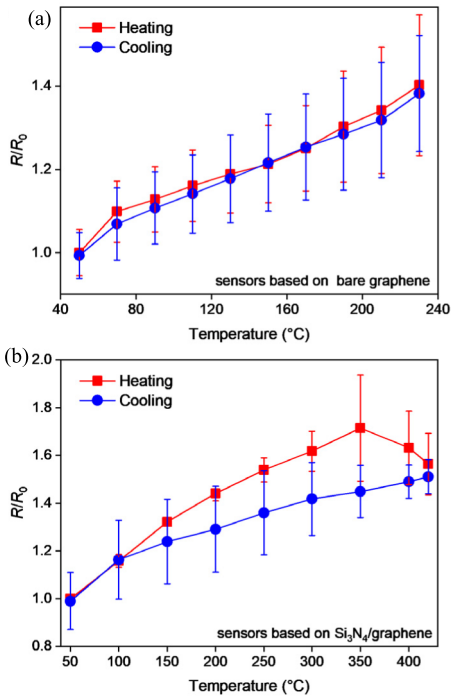

Fig. 3. Comparison of the temperature characteristic curves of the graphene pressure sensors with and without Si_3N_4 protection. (a) Variation in normalized resistance of the pressure sensors based on bare graphene against the temperature ranges from 50 °C to 230 °C. (b) Variation in normalized resistance of the pressure sensors based on Si_3N_4/graphene against the temperature ranges from 50 °C to 420 °C.

temperature increases, the interaction between electrons and lattice vibration is enhanced, and the mobility of carrier is reduced, leading to the decrease in graphene resistance [35]. The thermal expansion effect refers to the thermal expansion of the gas in the micro cavity, which exert a thermal stress on the graphene, resulting in an increase in graphene resistance. In addition, the thermal expansion coefficient of graphene is different from that of the Si_3N_4 layer at the top, and thermal strain is also formed inside the graphene [36]. Under the influence of temperature, the resistance increase trend caused by thermal expansion is more significant than the resistance decrease trend caused by electron–phonon coupling, leading to the increase in resistance of both kinds of sensors. Similar results were shown in the research by Fang et al. [37]. The TCR is defined as the relative change of resistance when the temperature changes 1 °C, expressed as follows [38]:

$$\mathrm{TCR} = \frac{R - R_0}{R_0 \times \Delta T} \tag{1}$$

where R is the real-time resistance under the test temperature, R_0 is the resistance under the initial temperature, and ΔT is the temperature change. The TCR of the bare graphene pressure sensor is calculated as 0.224% °C^{-1} at 230 °C. When the graphene is coated with a Si_3N_4 protective layer, as the temperature rises to 350 °C, the electron–phonon coupling is more significant than the thermal expansion effect, causing the resistance of graphene to decline. The maximum TCR is 0.322% °C^{-1} at 150 °C [Fig. 3(b)], which is higher than that of the bare graphene pressure sensor, indicating an excellent performance under high temperatures.

After comparing the temperature characteristics of the graphene pressure sensors with and without Si_3N_4 protection,

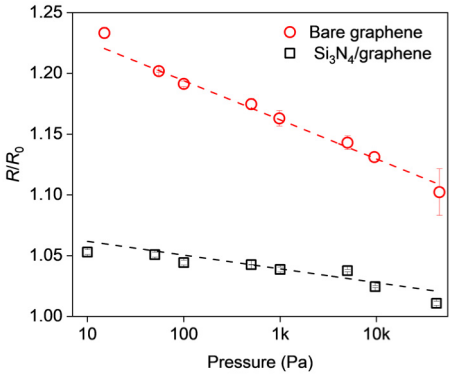

Fig. 4. Comparison of the piezoresistive characteristics of the graphene pressure sensor with and without Si_3N_4 protection at room temperature.

we further compared their piezoresistive characteristics at room temperature, as shown in Fig. 4. It can be seen that both sensors resistance increases as the pressure decreases. The reason is that when a pressure is applied, a pressure difference between the inside and outside of the rectangular cavity is formed, causing the mechanical bending and strain in the graphene. This means that the external pressure breaks the equilibrium state of the graphene lattice structure, which makes the conduction and valence bands of the graphene originally tangent open an energy gap at the Dirac point. The generation of the energy gap would greatly reduce the carrier mobility within the graphene, resulting in an increase in its resistance [39]. Since graphene exhibits this stress-induced piezoresistive effect, it is considered as a suitable force-sensitive material for pressure sensors.

The sensitivity of the pressure sensor based on the piezoresistive effect can be expressed as follows [13]:

$$S = \frac{R - R_0}{R_0 \times \Delta P} \tag{2}$$

where R is the real-time resistances of the graphene pressure sensor, R_0 is the initial resistance, and ΔP is the pressure difference acting on the membrane. By analyzing the data in Fig. 4, the mechanical sensitivity of the graphene pressure sensor falls from 2.33×10^{-3} down to 5.3×10^{-4} kPa^{-1} after covered by the 100-nm Si_3N_4 layer. Due to the increase in the sensing film thickness, the maximum deformation of the same load decreases, and the stress decreases in graphene, leading to a lower sensitivity. Although the sensitivity of the sensor has decreased, the device still shows the good piezoresistive characteristics, and the maximum temperature tolerance of the sensor increases from 230 °C to 420 °C (Fig. 3). These results show that the Si_3N_4/graphene structure can be utilized as a pressure sensor with a high-temperature tolerance.

The effect of the rectangular cavity size on the mechanical properties of the membrane is also investigated. The resistance responses of the sensor when the pressure varies from 100 to 10 kPa with different rectangular cavity dimensions under room temperature are shown in Fig. 5. The dimensions of the cavity are 64 × 6, 64 × 9, and 64 × 12 μm^2, respectively. When the cavity size is 64 × 9 μm^2, an initial resistance of 1424 Ω is measured, and a largest resistance change of 5.3% is achieved when the pressure varies from 100 kPa down to 10 Pa. Hence, the highest sensitivity of 5.32×10^{-4} kPa^{-1} is obtained, which is better than other reported piezoresistive pressure sensors based on silicon [27], [28], carbon nanotubes [29], and graphene materials [13], [30], [31].

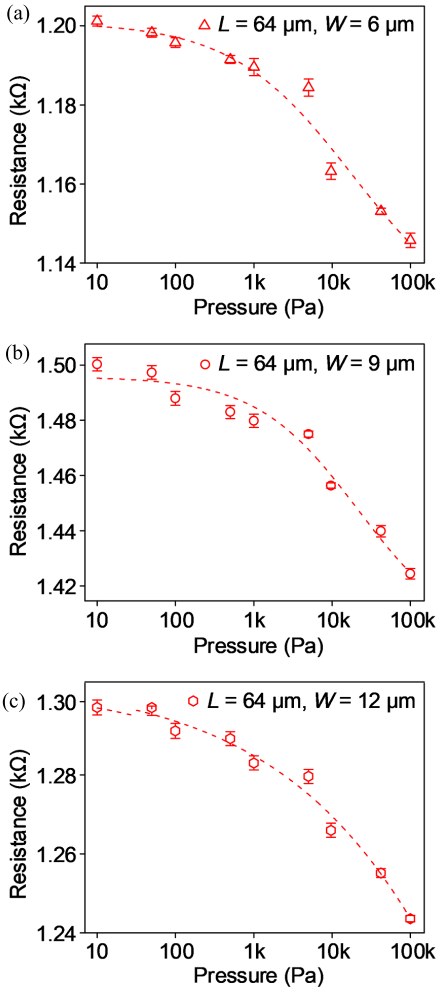

Fig. 5. Piezoresistive characteristics of three graphene pressure sensors with different rectangular cavity sizes at room temperature. (a) 64 × 6-μm^2 rectangular cavity. (b) 64 × 9-μm^2 rectangular cavity. (c) 64 × 12-μm^2 rectangular cavity.

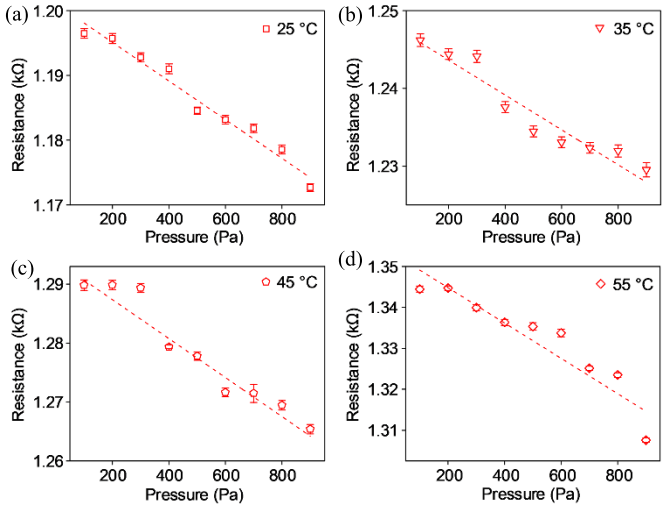

Fig. 6. Resistance of the graphene pressure sensor with pressure ranging from 100 to 900 Pa under different temperatures. (a) 25 °C. (b) 35 °C. (c) 45 °C. (d) 55 °C.

In order to investigate the influence of temperature on the sensitivity, the thermal control system was activated to continuously test the piezoresistive characteristics of the device from room temperature to 55 °C. Fig. 6 shows the resistance of the sensor from 100 to 900 Pa at different temperatures. At room temperature, the initial resistance of the device is measured as 1158 Ω, and the maximum sensitivity is calculated as 3.35 × 10^{-4} kPa^{-1}. From Fig. 6, it can be seen that as the temperature increases from 25 °C to 55 °C, the resistance of the graphene pressure sensor is positively correlated with the temperature and linearly negatively correlated with the pressure. When the external pressure is 500 Pa, the resistance at 55 °C shows a maximum relative change, which is 12.75% higher than that at 25 °C, and the TCR is 0.43% °C^{-1}. The slopes of the resistance–pressure curves are almost identical for all temperatures, indicating that the sensitivity of the device is less affected by the temperature between 25 °C and 55 °C. The performance comparisons between our graphene high-temperature pressure sensor with a Si_3N_4 protective layer and other pressure sensors are shown in Table I. Among all the listed pressure sensors, our sensor shows the highest sensitivity.

TABLE I
PERFORMANCE COMPARISON AMONG THE PRESSURE SENSORS

Device structure	Sensitivity (kPa^{-1})	Temperature range (°C)	Reference
Si_3N_4/graphene	5.32×10^{-4}	25~55	This work
Graphene on SiN_x	2.8×10^{-4}	23~70	[40]
BN/graphene/BN	1.87×10^{-4}	30~180	[14]
Suspended graphene	2.96×10^{-5}	RT	[13]
Carbon nanotubes	1.06×10^{-5}	RT	[29]
Boron doped silicon	3.2×10^{-5}	RT	[28]
Aluminum-Silicon	2.83×10^{-4}	-20~50	[41]
SOI	2.10 ×10^{-4}	20~220	[42]

IV. CONCLUSION

In this article, we introduced a novel graphene high-temperature pressure sensor with a Si_3N_4 protective layer, which exhibits excellent performance under different pressures. Because of the well-protected Si_3N_4, which provides stable protection for the sensitive graphene layer, the fabricated sensor can sustain good electrical characteristics under high temperatures up to 420 °C. The thickness of the protective layer can be increased, or the material can be replaced to obtain sensors that can adapt to various extreme environments. The resistance of the obtained sensor increases as pressure decreases, and a sensitivity of around 5.32 × 10^{-4} kPa^{-1} is obtained at room temperature. It is worth noting that the reported performance is better than the conventional pressure sensors based on silicon and carbon tubes. It is believed that our proposed graphene high-temperature pressure sensor with a Si_3N_4 protective layer has good potential in petrochemical, automotive electronics, and other fields.

ACKNOWLEDGMENT

The authors would like to thank the teachers of the laboratory instrument in the Institute of Microelectronics, Tsinghua University, Beijing, China, such as Li Zong, Bing Han, Zhonghui Zhang, Xin Su, Yuxia Fu, Wenwen Jia, and Peng Liu, for their help on the device fabrication and pressure measurement.

REFERENCES

[1] W. Zhang, S. Yao, S. Zhang, Y. Liu, and H. Qu, "Status quo of high-temperature pressure sensor and its prospect," *Instrum. Technique Sensor*, vol. 4, pp. 6–8, Apr. 2002, doi: 10.3969/j.issn.1002-1841.2002.04.003.

[2] J. Zhou, Z. Hou, and D. Xiao, "Review on pressure sensors in harsh environment," *Nat. Defense Sci. Technol.*, vol. 36, no. 4, pp. 15–19, Aug. 2015, doi: 10.13943/j.issn.1671-4547.2015.04.04.

[3] K. I. Bolotin et al., "Ultrahigh electron mobility in suspended graphene," *Solid State Commun.*, vol. 146, no. 9, pp. 351–355, Feb. 2008, doi: 10.1016/j.ssc.2008.02.024.

[4] J. M. Dawlaty, S. Shivaraman, M. Chandrashekhar, M. G. Spencer, and F. Rana, "Measurement of ultrafast carrier dynamics in epitaxial graphene," *MRS Proc.*, vol. 1081, p. 41116, Jan. 2008, doi: 10.1557/proc-1081-p06-04.

[5] A. A. Balandin et al., "Superior thermal conductivity of single-layer graphene," *Nano Lett.*, vol. 8, no. 3, pp. 902–907, Apr. 2008, doi: 10.1021/nl0731872.

[6] C. Lee, X. Wei, J. W. Kysar, and J. Hone, "Measurement of the elastic properties and intrinsic strength of monolayer graphene," *Science*, vol. 321, no. 5887, pp. 385–388, Jul. 2008, doi: 10.1126/science.1156211.

[7] F. Liu, P. Ming, and J. Li, "*Ab initio* calculation of ideal strength and phonon instability of graphene under tension," *Phys. Rev. B, Condens. Matter*, vol. 76, no. 6, Aug. 2007, Art. no. 064120, doi: 10.1103/PhysRevB.76.064120.

[8] V. M. Pereira, A. H. C. Neto, and N. M. R. Peres, "Tight-binding approach to uniaxial strain in graphene," *Phys. Rev. B, Condens. Matter*, vol. 80, no. 4, p. 45401, Jul. 2009, doi: 10.1103/PhysRevB.80.045401.

[9] J. S. Bunch et al., "Impermeable atomic membranes from graphene sheets," *Nano Lett.*, vol. 8, no. 8, pp. 2458–2462, Aug. 2008, doi: 10.1021/nl801457b.

[10] Q. Shao, G. Liu, D. Teweldebrhan, and A. A. Balandin, "High-temperature quenching of electrical resistance in graphene interconnects," *Appl. Phys. Lett.*, vol. 92, no. 20, May 2008, Art. no. 202108, doi: 10.1063/1.2927371.

[11] F. Schedin et al., "Detection of individual gas molecules adsorbed on graphene," *Nature Mater.*, vol. 6, pp. 652–655, Jul. 2007, doi: 10.1038/nmat1967.

[12] J. S. Bunch et al., "Electromechanical resonators from graphene sheets," *Science*, vol. 315, no. 5811, pp. 490–493, Feb. 2007, doi: 10.1126/science.1136836.

[13] A. D. Smith et al., "Electromechanical piezoresistive sensing in suspended graphene membranes," *Nano Lett.*, vol. 13, no. 7, pp. 3237–3242, Jul. 2013, doi: 10.1021/nl401352k.

[14] M. Li et al., "Pressure sensing element based on the BN-graphene-BN heterostructure," *Appl. Phys. Lett.*, vol. 112, no. 14, Apr. 2018, Art. no. 143502, doi: 10.1063/1.5017079.

[15] M. Li, T. Zhang, P. Wang, M. Li, J. Wang, and Z. Liu, "Temperature characteristics of a pressure sensor based on BN/graphene/BN heterostructure," *Sensors*, vol. 19, no. 10, p. 2223, May 2019, doi: 10.3390/s19102223.

[16] Z. G. Wang et al., "Effects of methane flux on structural and transport properties of CVD-grown graphene films," *Vacuum*, vol. 86, no. 7, pp. 895–898, Feb. 2012, doi: 10.1016/j.vacuum.2011.05.011.

[17] A. Srivastava et al., "Novel liquid precursor-based facile synthesis of large-area continuous, single, and few-layer graphene films," *Chem. Mat.*, vol. 22, no. 11, pp. 3457–3461, May 2010, doi: 10.1021/cm101027c.

[18] H. H. Kim, Y. Chung, E. Lee, S. K. Lee, and K. Cho, "Water-free transfer method for CVD-grown graphene and its application to flexible air-stable graphene transistors," *Adv. Mater.*, vol. 26, no. 20, pp. 3213–3217, May 2014, doi: 10.1002/adma.201305940.

[19] H. K. Seo, M. H. Park, Y. H. Kim, S. J. Kwon, S. H. Jeong, and T. W. Lee, "Laminated graphene films for flexible transparent thin film encapsulation," *ACS Appl. Mater. Interface*, vol. 8, no. 23, pp. 14725–14731, Jun. 2016, doi: 10.1021/acsami.6b01639.

[20] C. T. Phare, Y.-H. D. Lee, J. Cardenas, and M. Lipson, "Graphene electro-optic modulator with 30 GHz bandwidth," *Nature Photon.*, vol. 9, no. 8, pp. 511–514, Jul. 2015, doi: 10.1038/nphoton.2015.122.

[21] Y. Koh, H. Kim, H. Kim, and J. W. Halloran, "Thermal shock resistance of fibrous monolithic Si_3N_4/BN ceramics," *J. Eur. Ceram. Soc.*, vol. 24, no. 8, pp. 2339–2347, Jul. 2004, doi: 10.1016/S0955-2219(03)00644-7.

[22] Z. Wang et al., "Air-stable n-type doping of graphene from overlying Si_3N_4 film," *Appl. Surf. Sci.*, vol. 307, pp. 712–715, Jul. 2014, doi: 10.1016/j.apsusc.2014.04.107.

[23] H. Li, Q. Zhang, C. Liu, S. Xu, and P. Gao, "Ambipolar to unipolar conversion in graphene field-effect transistors," *ACS Nano*, vol. 5, no. 4, pp. 3198–3203, Mar. 2011, doi: 10.1021/nn200327q.

[24] R. C. C. Yap, H. Li, W. L. Chow, C. X. Lu, B. K. Tay, and E. H. T. Teo, "Identifying the mechanisms of p-to-n conversion in unipolar graphene field-effect transistors," *Nanotechnology*, vol. 24, no. 19, Apr. 2013, Art. no. 195202, doi: 10.1088/0957-4484/24/19/195202.

[25] F. Su, Z. Zhang, S. Li, P. Li, and T. Deng, "Long-term stability of photodetectors based on graphene field-effect transistors encapsulated with Si3N4 layers," *Appl. Surf. Sci.*, vol. 459, pp. 164–170, Nov. 2018, doi: 10.1016/j.apsusc.2018.07.208.

[26] D. Geng et al., "Nitrogen doping effects on the structure of graphene," *Appl. Surf. Sci.*, vol. 257, no. 21, pp. 9193–9198, Aug. 2011, doi: 10.1016/j.apsusc.2011.05.131.

[27] L. Yang, L. Yang, C. Lai, C. Dai, and P. Chang, "A piezoresistive micro pressure sensor fabricated by commercial DPDM CMOS process," *J. Appl. Sci. Eng.*, vol. 8, no. 1, pp. 67–73, Mar. 2005, doi: 10.6180/jase.2005.8.1.09.

[28] Y. Zhang, C. Yang, Z. Zhang, H. Lin, L. Liu, and T. Ren, "A novel pressure microsensor with 30-μm-thick diaphragm and meander-shaped piezoresistors partially distributed on high-stress bulk silicon region," *IEEE Sensors J.*, vol. 7, no. 12, pp. 1742–1748, Nov. 2007, doi: 10.1109/JSEN.2007.910298.

[29] C. Hierold, A. Jungen, C. Stampfer, and T. Helbling, "Nano electromechanical sensors based on carbon nanotubes," *Sens. Actuators A, Phys.*, vol. 136, no. 1, pp. 51–61, May 2007, doi: 10.1016/j.sna.2007.02.007.

[30] A. M. Hurst, S. Lee, N. Petrone, J. VanDeWeert, A. M. Van Der Zande, and J. Hone, "A transconductive graphene pressure sensor," in *Proc. 17th Int. Conf. Solid-State Sensors, Actuators Microsyst. (TRANSDUCERS & EUROSENSORS XXVII)*, Jun. 2013, pp. 586–589.

[31] S.-E. Zhu, M. K. Ghatkesar, C. Zhang, and G. C. A. M. Janssen, "Graphene based piezoresistive pressure sensor," *Appl. Phys. Lett.*, vol. 102, no. 16, Apr. 2013, Art. no. 161904, doi: 10.1063/1.4802799.

[32] L. M. Malard, M. A. Pimenta, G. Dresselhaus, and M. S. Dresselhaus, "Raman spectroscopy in graphene," *Phys. Rep.*, vol. 473, no. 5, pp. 51–87, Mar. 2009, doi: 10.1016/j.physrep.2009.02.003.

[33] S.-I. Kobayashi, "IR spectroscopic study of silicon nitride films grown at a low substrate temperature using very high frequency plasma-enhanced chemical vapor deposition," *World J. Condens. Matter Phys.*, vol. 6, no. 4, pp. 287–293, 2016, doi: 10.4236/wjcmp.2016.64027.

[34] L. S. Panchakarla et al., "Synthesis, structure, and properties of boron- and nitrogen-doped graphene," *Adv. Mater.*, vol. 21, pp. 4726–4730, Aug. 2009, doi: 10.1002/adma.200901285.

[35] D. K. Linh and N. Q. Khanh, "Electrical conductivity of bilayer-graphene double layers at finite temperature," *Superlattices Microstructures*, vol. 114, pp. 406–415, Feb. 2018, doi: 10.1016/j.spmi.2018.01.006.

[36] S. Wang, M. Tambraparni, J. Qiu, J. Tipton, and D. Dean, "Thermal expansion of graphene composites," *Macromolecules*, vol. 42, no. 14, pp. 5251–5255, Jul. 2009, doi: 10.1021/ma900631c.

[37] Y. Fang, Y. Zhang, Y. Li, J. Sun, M. Zhu, and T. Deng, "A novel temperature sensor based on three-dimensional buried-gate graphene field effect transistor," *Nanotechnology*, vol. 32, no. 48, Nov. 2021, Art. no. 485505, doi: 10.1088/1361-6528/ac1f53.

[38] X. Zhao, Y. Long, T. Yang, J. Li, and H. Zhu, "Simultaneous high sensitivity sensing of temperature and humidity with graphene woven fabrics," *ACS Appl. Mater. Interfaces*, vol. 9, no. 35, pp. 30171–30176, Aug. 2017, doi: 10.1021/acsami.7b09184.

[39] A. D. Smith et al., "Pressure sensors based on suspended graphene membranes," *Solid-State Electron.*, vol. 88, pp. 89–94, Oct. 2013, doi: 10.1016/j.sse.2013.04.019.

[40] Q. Wang, W. Hong, and L. Dong, "Graphene 'microdrum' on a freestanding perforated thin membrane for high sensitivity MEMS pressure sensors," *Nanoscale*, vol. 8, no. 14, pp. 7663–7671, Mar. 2016, doi: 10.1039/c5nr09274d.

[41] X. Xie, J. Zhang, M. Li, Q. Liu, and X. Mao, "Design and fabrication of temperature-insensitive MEMS pressure sensor utilizing aluminum-silicon hybrid structures," *IEEE Sensors J.*, vol. 21, no. 5, pp. 5861–5870, Mar. 2021, doi: 10.1109/JSEN.2020.3040742.

[42] Z. Yao et al., "Passive resistor temperature compensation for a high-temperature piezoresistive pressure sensor," *Sensors*, vol. 16, no. 7, p. 1142, Jul. 2016, doi: 10.3390/s16071142.